Insights into exo- and endoglucanase activities of family 6 glycoside hydrolases from Podospora anserina

Laetitia Poidevin, Julia Feliu, Annick Doan, Jean-Guy Berrin, Mathieu Bey, Pedro M Coutinho, Bernard Henrissat, Eric Record, Senta Heiss-Blanquet

Applied and Environmental Microbiology

Insights into Exo- and Endoglucanase Activities of Family 6 Glycoside Hydrolases from Podospora anserina

Laetitia Poidevin, Julia Feliu, Annick Doan, Jean-Guy Berrin, Mathieu Bey, Pedro M. Coutinho, Bernard Henrissat, Eric Record and Senta Heiss-Blanquet

Appl. Environ. Microbiol. **2013, 79(14):4220. DOI: 10.1128/AEM.00327-13.**
Published Ahead of Print 3 May 2013.

AEM
Journals.ASM.org

Insights into Exo- and Endoglucanase Activities of Family 6 Glycoside Hydrolases from *Podospora anserina*

Laetitia Poidevin,[a,b]* Julia Feliu,[b] Annick Doan,[b] Jean-Guy Berrin,[b] Mathieu Bey,[b] Pedro M. Coutinho,[c] Bernard Henrissat,[c] Eric Record,[b] Senta Heiss-Blanquet[a]

IFP Energies Nouvelles, Rueil-Malmaison, France[a]; INRA, Aix-Marseille Université, UMR 1163 de Biotechnologie des Champignons Filamenteux, Polytech, Marseille, France[b]; Architecture et Fonction des Macromolécules Biologiques, Aix-Marseille Université, CNRS UMR 7257, Marseille, France[c]

The ascomycete *Podospora anserina* is a coprophilous fungus that grows at late stages on droppings of herbivores. Its genome encodes a large diversity of carbohydrate-active enzymes. Among them, four genes encode glycoside hydrolases from family 6 (GH6), the members of which comprise putative endoglucanases and exoglucanases, some of them exerting important functions for biomass degradation in fungi. Therefore, this family was selected for functional analysis. Three of the enzymes, *P. anserina* Cel6A (*Pa*Cel6A), *Pa*Cel6B, and *Pa*Cel6C, were functionally expressed in the yeast *Pichia pastoris*. All three GH6 enzymes hydrolyzed crystalline and amorphous cellulose but were inactive on hydroxyethyl cellulose, mannan, galactomannan, xyloglucan, arabinoxylan, arabinan, xylan, and pectin. *Pa*Cel6A had a catalytic efficiency on cellotetraose comparable to that of *Trichoderma reesei* Cel6A (*Tr*Cel6A), but *Pa*Cel6B and *Pa*Cel6C were clearly less efficient. *Pa*Cel6A was the enzyme with the highest stability at 45°C, while *Pa*Cel6C was the least stable enzyme, losing more than 50% of its activity after incubation at temperatures above 30°C for 24 h. In contrast to *Tr*Cel6A, all three studied *P. anserina* GH6 cellulases were stable over a wide range of pHs and conserved high activity at pH values of up to 9. Each enzyme displayed a distinct substrate and product profile, highlighting different modes of action, with *Pa*Cel6A being the enzyme most similar to *Tr*Cel6A. *Pa*Cel6B was the only enzyme with higher specific activity on carboxymethylcellulose (CMC) than on Avicel and showed lower processivity than the others. Structural modeling predicts an open catalytic cleft, suggesting that *Pa*Cel6B is an endoglucanase.

Cellulose, a polysaccharide of β-1,4-linked D-glucose units, is the most abundant biopolymer on earth. It is the main constituent of plant cell walls, where it forms a tight complex together with hemicelluloses and is embedded in the lignin matrix. Cellulose is a recalcitrant material organized into microfibrils and composed of highly ordered glucan chains interlinked by hydrogen bonds. Depending on the source of cellulose, these fibrils have a more or less crystalline character, and for deconstruction of these complex structures, microorganisms have developed specialized enzymatic systems. All cellulolytic organisms produce multiple enzymes for cellulose degradation, but three main catalytic activities are necessary for complete hydrolysis: exoglucanases (or cellobiohydrolases [CBHs]) attack cellulose chains from the chain ends, and endoglucanases cleave the cellulose chain randomly, while β-glucosidases hydrolyze cellobiose, the reaction product of cellobiohydrolases. For efficient degradation, all three enzymatic activities have to be present, and synergistic interactions have been shown to be essential for a rapid degradation process (1–4). While exo-endo synergy can be easily explained by endoglucanases creating new chain ends for exoglucanases, exo-exo synergy still lacks a fully satisfactory explanation.

In contrast to synergistic interactions, the reaction mechanism of isolated enzymes is better understood, since structure-function studies have led to the identification of catalytic residues for cellobiohydrolases and endoglucanases (5–11). Sequence similarity and, therefore, structural properties are at the origin of the classification of these enzymes in the CAZy (Carbohydrate-Active enZymes) database, facilitating the assignment of function (12). Fungal endoglucanases are classified into glycoside hydrolase families GH5, GH6, GH7, GH9, GH12, GH45, and GH74, while fungal exoglucanases can be found in families GH6, GH7, and GH48.

At the three-dimensional (3D) level, cellobiohydrolases are characterized by a typical tunnel-shaped active site, with the roof of the tunnel formed by long flexible loops (5, 13–15). In contrast, their homologous endoglucanases bear shorter loops converting their active site into a classical cleft. This difference in active-site topology has consequences in the action pattern of the enzymes. The cellulose chain end is believed to enter the tunnel active site of cellobiohydrolases and to be cut processively into cellobiose units as it threads through the tunnel (5, 16). Instead, the open cleft active site of endoglucanases is thought to allow random binding and cleavage along the cellulose chain.

An increasing number of genomic and proteomic studies on fungi reveal a large variety of lignocellulose-degrading enzymes present in these organisms. A very interesting ascomycete is *Podospora anserina*, which grows on herbivore dung. Its mycelium develops at a late stage, after the most easily utilizable biomass components, such as hemicellulose and pectin, have already been degraded by other species. *P. anserina* is therefore hypothesized to be able to specifically use the recalcitrant parts of lignocellulose. The analysis of its genome has indeed revealed an impressive number of genes encoding carbohydrate-activating enzymes (CAZymes) and enzymes putatively involved in lignin degradation, including oxidoreductases, cellobiose dehydrogenase, cop-

Received 29 January 2013 **Accepted** 25 April 2013
Published ahead of print 3 May 2013
Address correspondence to Senta Heiss-Blanquet, senta.blanquet@ifpen.fr.
* Present address: Laetitia Poidevin, Department of Plant Pathology and Microbiology, University of California, Riverside, California, USA.

doi:10.1128/AEM.00327-13

per radical oxidases, or laccases, which is a rather atypical feature for ascomycetes (17). The total number of putative glycoside hydrolases is similar to those in other sequenced ascomycetes, but it has the largest panel of cellulose-degrading enzymes and carbohydrate binding modules (CBMs). For instance, *P. anserina* has 30 genes encoding putative cellulases belonging to the families cited above, compared to only 8 for *Trichoderma reesei*, a number which is particularly small compared to most other carbohydrate-degrading ascomycetes (18).

The specific activity of CBHs on soluble and insoluble substrates has been shown to be lower than that of endoglucanases (19), and the CBH activity is probably rate limiting for cellulose hydrolysis (20). For efficient hydrolysis, a large amount of CBH enzyme is therefore needed in cellulolytic complexes, such as the one of *T. reesei*. In the latter organism, CBHs are the most abundant enzymes; i.e., Cel7A (CBH1) makes up 40 to 60% and Cel6A (CBH2) makes up about 20 to 30% of the total amount of secreted proteins (21). An enhancement of Cel6A was shown to be beneficial for hydrolytic activity of the complex (22), and Cel6A deletion mutants showed a 33% decrease in saccharification efficiency (23). Intriguingly, *T. reesei* contains only one enzyme of the GH6 family, in contrast to *Humicola insolens* and *Myceliophthora thermophila*, two other fungi that produce efficient cellulolytic cocktails containing three family GH6 enzymes. *H. insolens* Cel6A and Cel6B have been shown to display endoglucanase and cellobiohydrolase activities, respectively (24–26). *P. anserina* has four genes encoding putative GH6 enzymes, but to date, nothing is known about the enzymatic properties of this important family of cellulose-degrading enzymes in this organism. The reason for the existence of multiple enzymes is not known, and the question arises as to whether there is redundancy or if each enzyme has a distinct role.

To answer this question, we undertook the cloning of the four *P. anserina* genes encoding putative GH6 cellulases to express them heterologously. We successfully produced three of the enzymes, termed *P. anserina* Cel6A (*Pa*Cel6A), *Pa*Cel6B, and *Pa*Cel6C. Substrate and product profiles of the purified enzymes revealed significant differences concerning the specificities and modes of action on cellulose model substrates. The biochemical characteristics of *P. anserina* GH6 cellulases were compared to those of *T. reesei* Cel6A (*Tr*Cel6A), revealing differences in their modes of action.

MATERIALS AND METHODS

Culture media. *P. anserina* was grown at 27°C on M2 medium, composed of 0.25 g liter^{-1} KH_2PO_4, 0.3 g liter^{-1} K_2HPO_4, 0.25 g liter^{-1} $MgSO_4 \cdot 7H_2O$, 0.5 g liter^{-1} urea, 0.05 g liter^{-1} thiamine, 0.25 g liter^{-1} biotin, 2.5 mg liter^{-1} citric acid, 2.5 mg liter^{-1} $ZnSO_4$, 0.5 mg liter^{-1} $CuSO_4$, 125 μg liter^{-1} $MnSO_4$, 25 μg liter^{-1} boric acid, 25 μg liter^{-1} Na_2MoO_4, 25 μg liter^{-1} iron alum, 5 g liter^{-1} dextrin, and 10 g liter^{-1} yeast extract, adjusted to pH 7.0 with KH_2PO_4. For *Pichia pastoris*, three media were used: minimum methanol (MM), composed of 3.4 g liter^{-1} yeast nitrogen base (YNB) (Difco), 10 g liter^{-1} ammonium sulfate, 20 g liter^{-1} agar, 2 ml of 200 g liter^{-1} biotin, and 5 ml of pure methanol; BMGY, containing 3.4 g liter^{-1} YNB, 10 g liter^{-1} ammonium sulfate, 10 g liter^{-1} glycerol, 10 g liter^{-1} yeast extract, 10 g liter^{-1} peptone, 100 ml of 1 M phosphate buffer (pH 6.0), and 2 ml of 200 g liter^{-1} biotin; and BMMY, which is identical to BMGY except that it contains 30 ml liter^{-1} of pure methanol instead of glycerol.

Cloning procedures. *P. anserina* strain S mat+, which was used in this study, was kindly provided by P. Silar (CNRS, Paris, France). *P. anserina* cells were grown in baffled flasks at 120 rpm and at 27°C on M2 medium (0.25 g liter^{-1} KH_2PO_4, 0.3 g liter^{-1} K_2HPO_4, 0.25 g liter^{-1} $MgSO_4 \cdot 7H_2O$, 0.5 g liter^{-1} urea, 0.05 mg liter^{-1} thiamine, 0.25 μg liter^{-1} biotin, 2.5 mg liter^{-1} citric acid, 2.5 mg liter^{-1} $ZnSO_4$, 0.5 mg liter^{-1} $CuSO_4$, 125 μg liter^{-1} $MnSO_4$, 25 μg liter^{-1} boric acid, 25 μg liter^{-1} Na_2MoO_4, 25 μg liter^{-1} iron alum, 5 g liter^{-1} dextrin [pH 7]) supplemented with 1% Avicel cellulose, with or without induction by 0.1% sophorose 1 h prior to harvesting of the mycelia. Total RNA was extracted from 3- or 5-day-old cultures with the RNeasy plant kit (Qiagen, Courtaboeuf, France), and cDNAs were synthesized by using SuperScript reverse transcriptase (RT) (Life Technologies, NY, USA), according to the manufacturer's instructions. *Pa*Cel6B and *Pa*Cel6D were amplified by PCR using *Pfu* DNA polymerase (Promega, WI, USA) and the following primers: *PaCel6B*-F (5′-TAG AAT TCG CCC CTT CCC CGA CCA CC-3′), *PaCel6B*-R (5′-GAT CTA GAC CGA GAA GGG AAG GGT TAG A-3′), *PaCel6D*-F (5′-TAG AAT TCT CTC CCC TTG AGG CAC GC-3′), and *PaCel6D*-R (5′-GAT CTA GAC CCA AGC ACT GCG AAT ACC A-3′). *Pa*Cel6A and *Pa*Cel6C could not be obtained by amplification, and their coding sequences were synthesized after codon optimization for expression in *P. pastoris* (Eurogentec, Belgium). The *Tr*Cel6A gene was amplified from cDNA obtained from *T. reesei* strain CL847. Coding sequences for *Pa*Cel6A, *Pa*Cel6B, *Pa*Cel6C, and *Tr*Cel6A were cloned into the pPICZαA vector (Life Technologies), in frame with the yeast α-secretion factor and with C-terminal hemagglutinin (HA) and His tags. For an unknown reason and despite multiple trials, the *Pa*Cel6D coding sequence, which was obtained after RT-PCR, could not be cloned into the expression vector and therefore could not be produced. The enzyme is therefore termed *Pa*GH6D.

Competent X33 yeast cells were prepared and transformed by electroporation according to the EasySelect Pichia expression kit protocol (Life Technologies). Expression vectors were linearized by PmeI (New England BioLabs, MA, USA) prior to transformation. After electroporation, cells were spread onto yeast extract-peptone-dextrose medium with sorbitol (YPDS)-zeocin plates. Transformants were selected by their lower growth rates on MM plates than on minimum dextrose (MD) plates.

Enzyme production and purification in *Pichia pastoris*. Culture supernatants of 10 clones were first analyzed by small-scale protein productions in a total volume of 10 ml BMGY, as described previously (27). When the optical density at 600 nm (OD_{600}) reached a value of between 2 and 6, cells were transferred into 2 ml BMMY and grown at 30°C, with daily addition of 3% (vol/vol) methanol. After SDS-PAGE analysis, clones with the highest secretion levels were selected, cultured in 200 ml BMGY starting culture, and transferred into 40 ml BMMY. Recombinant proteins were recovered after 5 days of methanol induction. After 10 min of centrifugation at 4,000 × *g*, supernatants were passed through a 0.2-μm filter. Samples were then concentrated 10 times in binding buffer (50 mM Tris-HCl [pH 7.8], 150 mM NaCl, 10 mM imidazole) by ultrafiltration in a Vivaspin 20 column (polyethersulfone membrane, 10-kDa cutoff; Sartorius, France). Subsequently, recombinant proteins were purified on a 5-ml HisTrap column (GE Healthcare) connected to an Äkta fast protein liquid chromatography (FPLC) apparatus (GE Healthcare), according to the manufacturer's instructions. Enzymes were eluted with binding buffer supplemented with 150 mM imidazole. A final ultrafiltration step was used to concentrate proteins in 50 mM acetate buffer (pH 5). Protein homogeneity was checked on a 12% SDS-polyacrylamide gel, followed by Coomassie staining.

Protein analysis. Deglycosylation of 2 μg recombinant protein was performed with 2 μl of either endo-α-*N*-acetylgalactosaminidase and 2 μl neuraminidase or 2 μl endoglycosidase H (Endo H) (all from New England BioLabs) for 2 h at 37°C, according to the manufacturer's instructions.

N-terminal sequences were determined by Edman degradation with a Procise cLC sequencing system (model 494cLC; Applied Biosystems) from purified protein samples electroblotted onto a polyvinylidene difluoride (PVDF) membrane (Life Technologies).

TABLE 1 Molecular characteristics of the four *P. anserina* GH6 enzymes and identities with known enzymes[a]

Enzyme	Gene ID[b]	Molecular mass (kDa) (pI) of encoded protein	CBM positions	Linker positions	Catalytic domain positions	No. of predicted glycosylation sites		% identity to *Tr*Cel6A (CBH2)[c]	Database entry with highest similarity, GenBank accession no. (% similarity)
						N-Glycosylation	*O*-Glycosylation		
*Pa*Cel6A	6187194	49.3 (5.8)	9–45	46–102	103–467	1	29	67.8	*Chaetomium globosum* hypothetical protein, EAQ82944 (77)
*Pa*Cel6B	6187311	41.3 (6.2)			1–364	3	2	35.4	*Myceliophthora thermophila* GH6, AEO57190 (73)
*Pa*Cel6C	6188027	40.9 (5.1)			1–380	1	3	45.8	*Sordaria macrospora* hypothetical protein, XP_003344888 (79)
*Pa*GH6D	6187939	44.0 (7.5)	377–412	349–376	1–348	1	9	35.0	*Humicola insolens* endoglucanase 6B, Q7SIG5 (82)

[a] Amino acid ranges of functional domains of mature proteins were predicted by InterproScan.
[b] Gene identifier as in the *P. anserina* reference genome sequence.
[c] Identity calculated with catalytic domains only.

Biochemical characterization by activity assays. Determinations of activity profiles on solid substrates were performed with microtiter plates by measuring the release of reducing sugars with 3,5-dinitrosalicylic acid (DNS), as reported previously (28). The total volume was 100 μl, containing 6.4 mg liter^{-1} of purified enzymes in 50 mM acetate buffer (pH 5) for *Tr*Cel6A or citrate-phosphate buffer (pH 7) for the three *Pa*Cel6 enzymes and 10 g liter^{-1} substrate. Substrates used were Avicel PH-101 cellulose, carboxymethylcellulose (CMC), hydroxyethyl cellulose (HEC), birchwood xylan, pectin (all from Sigma-Aldrich), barley β-glucan, 1,4-β-D-mannan, carob galactomannan, sugar beet arabinan, wheat arabinoxylan, arabinogalactan, xyloglucan, and konjak glucomannan (all from Megazyme, Wicklow, Ireland). Reaction mixtures were incubated at 35°C or 45°C, depending on enzyme stability, for 30 min. Reactions were stopped by boiling, and the mixtures were centrifuged at 4,000 × *g* for 3 min.

Activities on soluble cellooligosaccharides were measured at optimal pH and temperature with 20 mg/liter cellooligosaccharides and 10 mg liter^{-1} enzyme. Reactions were stopped after 30 min by placing the mixtures into boiling water for 5 min. Reaction products were analyzed with a Dionex ISC300 high-performance liquid chromatography (HPLC) system as described previously (29). For determination of kinetic constants, enzymes were incubated at an appropriate concentration (0.5 to 2 nM) in 50 mM phosphate buffer (pH 7) and at optimal temperature (45°C for *Pa*Cel6A and *Pa*Cel6B and 35°C for *Pa*Cel6C) with cellotetraose (0.5 to 30 μM) for up to 20 min. Reactions were inactivated by placing the mixtures into a boiling water bath for 5 min, and reaction products were analyzed by HPEAC-PAD (high-performance anion-exchange chromatography coupled with pulsed amperometric detection). Kinetic constants were determined by using the least-squares method.

Product profiles were established in duplicates on Avicel and CMC at 1% dry matter in 10 mM citrate-phosphate buffers. The substrates were incubated with 10 mg g^{-1} enzyme for 15 min and 24 h under optimal conditions (*Tr*Cel6A, 45°C at pH 5; *Pa*Cel6A, 45°C at pH 7; *Pa*Cel6B, 35°C at pH 7; *Pa*Cel6C, 25°C at pH 6). Reactions were stopped by boiling for 5 min, and reaction products (glucose, cellobiose, and cellotriose) were analyzed by HPEAC-PAD. Processivity was determined by using oligosaccharide ratios, as described previously (30, 31).

Effect of pH and temperature on enzymatic activity. The apparent optimal pH was estimated by using 1% Avicel in a total volume of 100 μl of 50 mM citrate-phosphate buffer (pH 3 to 7), 50 mM Tris-HCl (pH 7 to 9), and 50 mM Tris-maleate (pH 9 to 10). The optimal reaction temperature was studied by incubating the enzymes with 1% Avicel for 15 min at temperatures of between 30°C and 70°C, at pH 5 for *Tr*Cel6A and at pH 7 for *Pa*Cel6 enzymes. For enzymatic stabilities, enzymes were incubated in different buffers or at different temperatures for 24 h, and residual activity was measured as described above. Reducing sugars were determined according to a protocol adapted from a method described previously (32). Briefly, 40 μl of supernatant or glucose standard was added to 120 μl of reagent 1, made extemporarily from 2 volumes of reagent 1A [0.5 g liter^{-1} $K_3Fe(CN)_3$, 34.8 g liter^{-1} K_2HPO_4 (pH 10.6)] and 1 volume of reagent 1B (5.3 g liter^{-1} Na_2CO_3 and 0.65 g liter^{-1} KCN). The plates were sealed and heated to 96°C. After 10 min at room temperature, 80 μl of the reaction mix was added to 40 μl of reagent C (2.5 g liter^{-1} $FeCl_3$, 20 g liter^{-1} polyvinyl pyrrolidone K25, 2 N H_2SO_4). The optical density was measured at 520 nm after 15 min of incubation at room temperature in the dark. Each point was the mean of three independent measurements, with a standard deviation of 2 to 10%.

Cellulose binding assay. The capacity of adsorption of enzymes to Avicel was determined after incubating 60 μg of protein with 300 μl 1% Avicel PH-101 (Sigma-Aldrich) in 50 mM acetate buffer (pH 5) for *Tr*Cel6A or citrate-phosphate buffer (pH 7) for the three *Pa*Cel6 enzymes for 4 h at 4°C with agitation. After centrifugation, the amount of cellulases left in the supernatant was quantified by using the Bio-Rad protein assay kit with bovine serum albumin (BSA) as a standard (Bio-Rad, France). Controls without protein or with BSA were analyzed in parallel.

Structure modeling and bioinformatic analysis. Sequence alignments were done by using ClustalW on the EMBL-EBI server (http://www.ebi.ac.uk/Tools/msa/clustalw2/). *Pa*Cel6 structures were predicted by using the PHYRE2 server (http://www.sbg.bio.ic.ac.uk/phyre2/) (33). Models were visualized with PyMOL (PyMOL Molecular Graphics System, version 1.1; DeLano Scientific, USA). All *Pa*Cel6 models were registered in the Protein Model Database (http://www.caspur.it/PMDB/). PMDB identifiers are PM0077882, PM0077884, PM0077885, and PM0077886 for PaCel6A, PaCel6B, PaCel6C, and PaCel6D, respectively.

The NetOGlyc (http://www.cbs.dtu.dk/services/NetOGlyc/) and NetNGlyc (http://www.cbs.dtu.dk/services/NetNGlyc/) servers were used for glycosylation site predictions.

RESULTS

Sequence analysis and expression of *P. anserina* GH6 enzymes. The annotated *P. anserina* genome has four genes encoding family GH6 glycoside hydrolases (GenBank accession numbers XM_001903135 for *Pa*Cel6A, XM_001903174 for *Pa*Cel6B, XM_001903858 for *Pa*Cel6C, and XM_001903610 for *Pa*GH6D). *Pa*Cel6A and *Pa*GH6D both harbor a cellulose binding module of family CBM1 at their N terminus, explaining their slightly higher molecular masses (Table 1). *Pa*Cel6B, *Pa*Cel6C, and *Pa*GH6D catalytic domains have very limited identity to the *T. reesei* cellobiohydrolase 2 enzyme (*Tr*Cel6A).

At the time of writing, the most similar proteins that have been biochemically characterized are exoglucanase A from *Humicola insolens* (UniProtKB accession number Q9C1S9), displaying 72% and 50% identities to *Pa*Cel6A and *Pa*Cel6C, respectively, and *H. insolens* endoglucanase 6B (accession number Q7SIG5), with 54 and 82% identities to *Pa*Cel6B and *Pa*GH6D, respectively. Identities between the four *Pa*Cel6 enzymes ranged between 25 and 45%, with *Pa*Cel6B and *Pa*GH6D displaying the highest similarity

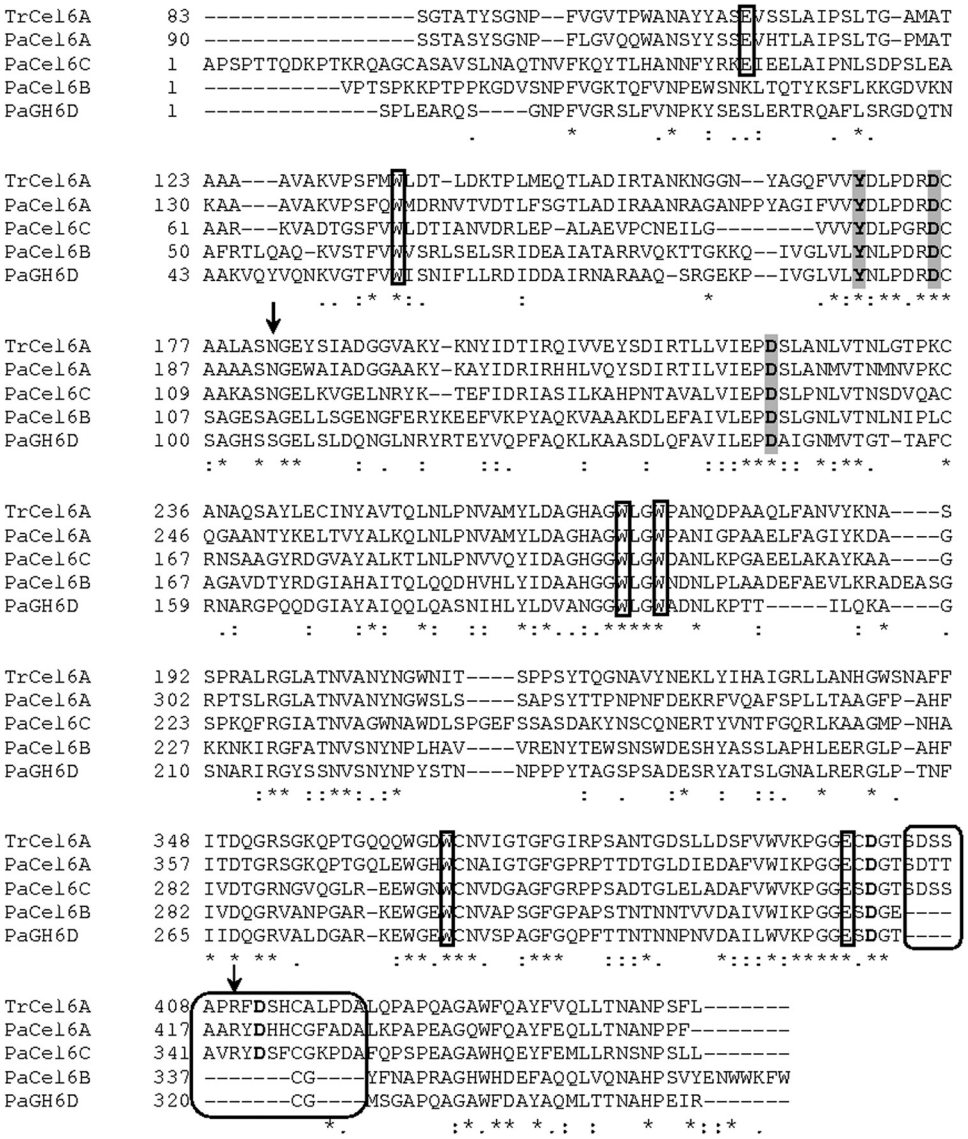

FIG 1 Amino acid sequence alignment of catalytic domains of *T. reesei* Cel6A and the four *P. anserina* family 6 glycoside hydrolases. Conserved residues are marked by an asterisk. Amino acids involved in catalysis are shaded. Amino acids implicated in glucose binding are boxed. Residues N182 and R410, which establish a direct contact between the two surface loops in *Tr*Cel6A, are indicated by an arrow. The sequence stretch corresponding to the second surface loop present in *Tr*Cel6A, *Pa*Cel6A, and *Pa*Cel6C, but absent in *Pa*Cel6B and *Pa*GH6D, is boxed.

to each other and *Pa*Cel6A and *Pa*GH6D displaying the lowest similarity.

Sequence analysis of the four *Pa*Cel6 enzymes was realized by a multiple alignment including *Tr*Cel6A (Fig. 1). All amino acids which are known to be involved in catalysis, namely, Asp221 (following *Tr*Cel6A numbering) and Asp175 (7), are conserved in all four *Pa*Cel6 sequences. Tyr169, proposed to participate in catalysis by causing distortion of the glucose ring undergoing catalysis (34), was also found to be conserved in all four proteins. Two other aspartic acid residues, Asp401 and Asp412, not directly involved in catalysis but contributing to full enzymatic activity (11), are conserved in *Pa*Cel6A and *Pa*Cel6C, but Asp412 is absent in *Pa*Cel6B and *Pa*GH6D. The most important amino acids involved in binding of the glucose moiety at the −2, +1, +2, and +4 subsites (throughout this paper, we follow the subsite nomenclature proposed by Davies et al. [35]) are also present in all four *Pa*Cel6 enzymes (Trp135, Trp269, Trp272, and Trp367) (9), but Glu107 (−3 subsite) is not conserved in *Pa*Cel6B and *Pa*GH6D (11).

In order to induce the expression of *Pa*Cel6 genes, *P. anserina* was grown on Avicel as the sole carbon source. Under this condition, only cDNAs encoding *Pa*Cel6B and *Pa*GH6D were obtained, whereas synthetic genes had to be generated for cloning of *Pa*Cel6A and *Pa*Cel6C in *P. pastoris*. For an unknown reason, cloning of the *Pa*GH6D coding sequence failed despite several trials, and the corresponding protein therefore could not be produced in *P. pastoris*. The three other proteins, *Pa*Cel6A, *Pa*Cel6B, and *Pa*Cel6C, finally yielded 30 to 130 mg liter^{-1} of protein after induction of *P. pastoris* transformants by methanol. In parallel, *Tr*Cel6A was also expressed in *P. pastoris* for comparative studies.

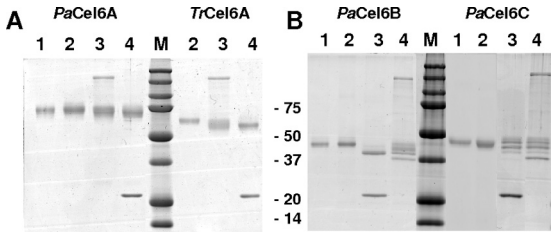

FIG 2 SDS-PAGE of Ni-purified recombinant glucanases. (A) *Pa*Cel6A and *Tr*Cel6A. Lanes 1 and 2, recombinant proteins; lanes 3, treatment with endo-α-*N*-acetylgalactosaminidase (*O*-glycosidase); lanes 4, treatment with Endo H. (B) *Pa*Cel6B and *Pa*Cel6C. Lanes 1 and 2, recombinant proteins; lanes 3, treatment with Endo H; lanes 4, treatment with endo-α-*N*-acetylgalactosaminidase (*O*-glycosidase). M, molecular mass marker (in kilodaltons) (Dual Precision Plus; Bio-Rad).

After purification on a Ni column, proteins were analyzed by SDS-PAGE (Fig. 2). All proteins displayed higher apparent molecular masses than the predicted ones, suggesting glycosylation by the host. Whereas *Pa*Cel6B and *Pa*Cel6C seemed only slightly glycosylated, *Pa*Cel6A and *Tr*Cel6A had an apparent molecular mass of about 70 kDa (theoretical mass of *Tr*Cel6A of 47.9 kDa). For all proteins, both *N*- and *O*-glycosylation sites are predicted (Table 1). Deglycosylation by Endo H led to reductions of the molecular masses of all proteins. The most important reduction was observed for *Tr*Cel6A and *Pa*Cel6B, which also have the largest number of predicted *N*-glycosylation sites (Fig. 2). A large number of *O*-glycosylation sites are predicted for the linker domain of *Tr*Cel6A and *Pa*Cel6A (Table 1). Treatment with endo-α-*N*-acetylgalactosaminidase reduced the molecular masses of all recombinant proteins. Several bands appeared after deglycosylation of *Pa*Cel6B and *Pa*Cel6C, which is supposed to be due to incomplete deglycosylation. The molecular mass of *Pa*Cel6A could not be reduced significantly by either *N*- or by *O*-deglycosylation. A lower level of incorporation of SDS or inefficient deglycosylation could explain the migration at a higher apparent molecular mass.

The N-terminal sequence was determined for all proteins, which confirmed that all of them were correctly processed, except for *Pa*Cel6A, which, for an unknown reason, lacked the first 5 amino acids. The N-terminal sequence of the mature protein started with ERQN. However, this should not impact the function of the CBM, which is situated at the N terminus, but is predicted to start only 8 amino acids further.

Enzymatic properties of *P. anserina* GH6 enzymes. *Pa*Cel6 enzymatic activities were assayed on cellooligosaccharides and structurally different polysaccharides. Table 2 summarizes the product profiles on G3 (cellotriose) to G6 (cellohexaose) cellodextrins. The observed cleavage pattern for *Tr*Cel6A confirmed previous results for the native enzyme (36). *Pa*Cel6 enzymes all had similar cleavage patterns, with the exception that glucose was never detected after cleavage by *Pa*Cel6A, in contrast to the three other enzymes. All enzymes were active on Avicel and CMC. In addition, *Pa*Cel6B displayed activity on barley β-(1,3;1,4)-glucan and glucomannan. No activity was detected on mannan, galactomannan, arabinoxylan, arabinan, xylan, xyloglucan, HEC, and pectin. As all enzymes were active on Avicel, this substrate was chosen to determine the apparent temperature and pH optima as well as stability. *Pa*Cel6 enzymes had rather narrow temperature optima, which were generally lower than that of *Tr*Cel6A. *Pa*Cel6A presented the highest activity at 55°C but had a 30%-lower activity at 65°C, in contrast to *Tr*Cel6A, which displayed the same activity at both temperatures (Fig. 3A). Temperature stability profiles showed that *Pa*Cel6A was the most stable of the *P. anserina* enzymes (up to 45°C, as for *Tr*Cel6A), whereas *Pa*Cel6B and *Pa*Cel6C lost nearly all activity after 24 h at 45°C and 35°C, respectively (Fig. 3B).

The Cel6 enzymes from *P. anserina* showed interesting activity profiles when the pH varied (Fig. 3C). These enzymes maintained nearly 100% of their activity from pH 5 up to pH 9, in contrast to *Tr*Cel6A, which lost about 50% of its activity at pH ≥6. Concerning stability, *Pa*Cel6A was also fairly stable for 24 h at these pH values. The activities of *Pa*Cel6B and *Pa*Cel6C declined upon incubation for 24 h at pH ≥7. The following experiments including the determination of kinetic parameters were conducted under optimal conditions for each enzyme.

Michaelis-Menten constants were determined on the soluble substrate cellotetraose. This substrate was cleaved by all four enzymes exclusively into two cellobiose units. HPAEC-PAD analyses revealed only traces of glucose and cellotriose. The kinetic behavior was very different for each *P. anserina* enzyme (Table 3). Kinetic constants for *Pa*Cel6A and *Tr*Cel6A were rather similar. The k_{cat} value of *Pa*Cel6A was 2-fold higher than that of *Tr*Cel6A, but it was determined at the optimal temperature for this enzyme (45°C), in contrast to *Tr*Cel6A (27°C). Interestingly, *Pa*Cel6B had a very high turnover number (k_{cat} = 27.7 s^{-1}) but the lowest affinity for cellotetraose (K_m = 43 μM). The k_{cat} of *Pa*Cel6C was about 100-fold lower than that of *Pa*Cel6B, but the affinity for cellotetraose was much higher. The catalytic efficiencies (k_{cat}/K_m) of *Pa*Cel6B and *Pa*Cel6C were 2-fold lower than those of *Pa*Cel6A and *Tr*Cel6A.

Product profile analyses. Because glycoside hydrolase family GH6 groups together both exo- and endoglucanases, we have determined the product profiles of the three *P. anserina* GH6 enzymes, using CMC and Avicel as substrates (Table 4). The main hydrolysis product from these cellulose substrates was cellobiose (G2) and, to a lesser extent, glucose (G1) and cellotriose (G3). The fact that *Tr*Cel6A slowly cleaves G3 leads to a larger amount of G3

TABLE 2 Product profile of recombinant *Pa*Cel6 enzymes and *Tr*Cel6A on soluble oligosaccharides

Enzyme	Substrate	Product(s)
*Tr*Cel6A	G3	G1, G2, G3
	G4	G2
	G5	G1, G2, G3
	G6	G1, G2, G3
*Pa*Cel6A	G3	G3
	G4	G2
	G5	G2, G3
	G6	G2, G3
*Pa*Cel6B	G3	G1, G2, G3
	G4	G2
	G5	G2, G3
	G6	G1, G2, G3
*Pa*Cel6C	G3	G1, G2, G3
	G4	G2
	G5	G2, G3
	G6	G2, G3

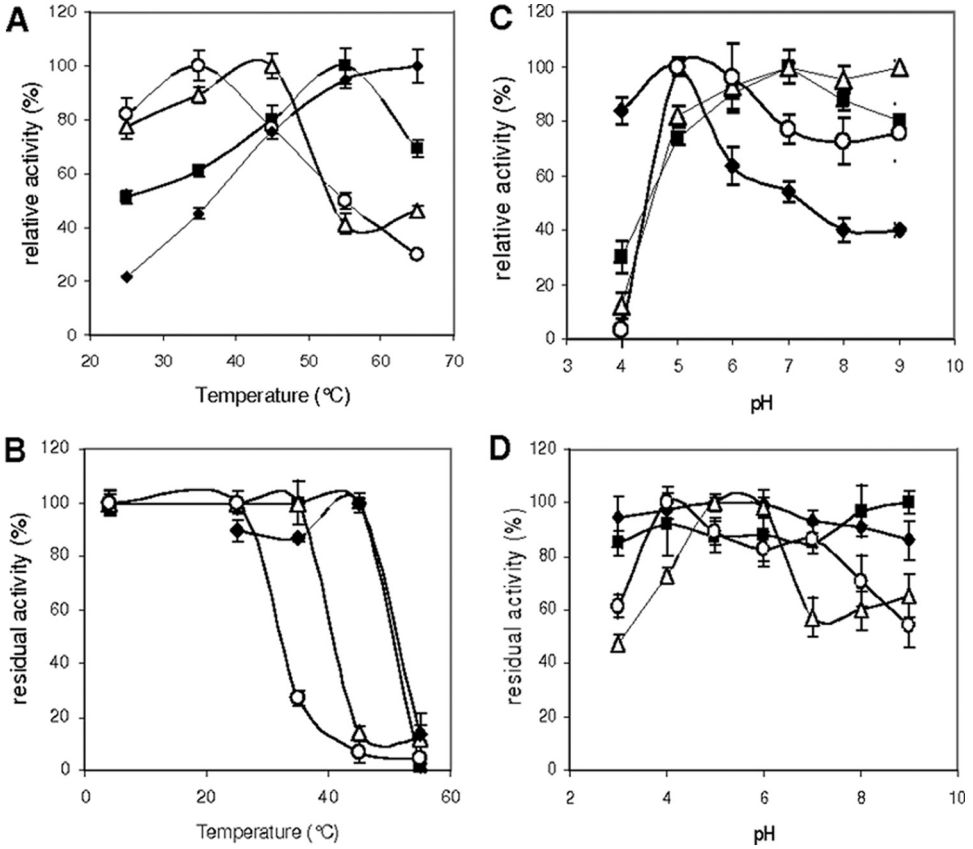

FIG 3 Activity of *P. anserina* Cel6 and *T. reesei* Cel6A on Avicel as a function of temperature and pH. (A) Optimal temperature. Avicel (1%) was hydrolyzed for 15 min at the indicated temperatures. (B) Temperature stability. Activity was measured after incubation at the indicated temperatures for 24 h. Hydrolysis reactions were conducted at 35°C. (C) Optimal pH. Hydrolysis reactions were conducted at 35°C for 15 min. (D) pH stability. Activity was measured at 35°C after incubation at the indicated pHs for 24 h. Symbols: filled diamonds, *Tr*Cel6A; filled squares, *Pa*Cel6A; open triangles, *Pa*Cel6B; open circles, *Pa*Cel6C. Values are means of triplicate measurements.

and lower G2/G3 ratios at 15 min than at 24 h. The G2/G1 ratio decreased slightly or remained the same at 24 h, which is in accordance with the formation of G1 following the cleavage of G3.

For *Pa*Cel6A, the G3 concentration increased from 6 to 49 μM between 15 min and 24 h, but the G2/G3 ratio increased at the same time. A similar trend was observed for G1; i.e., the glucose amounts and the G2/G1 ratio increased with time. These data suggest that G3 and G1 might be formed mainly in the first minutes of the reaction, by an initial attack liberating G1 or G3 instead of the G2 produced in a processive action ("false initial attack"

TABLE 3 Specific activities of recombinant enzymes on cellulose substrates and kinetic constants for *Pa*Cel6A, *Pa*Cel6B, and *Pa*Cel6C, compared to the constants for *Tr*Cel6A, measured on cellotetraose under optimal conditions for each enzyme

Enzyme	Sp act (nmol min^{-1} mg^{-1})		K_m (μM)	k_{cat} (s^{-1})	k_{cat}/K_m (μM^{-1} s^{-1})
	Avicel	CMC			
*Tr*Cel6A[a]	16.4	6.7	2.6	3.1	1.2
*Pa*Cel6A	7.6	3.0	4.7	6.6	1.4
*Pa*Cel6B	2.3	5.5	43.0	27.7	0.65
*Pa*Cel6C	1.9	1.1	0.59	0.3	0.54

[a] Kinetic constants reported previously (36), measured at 27°C and pH 5.

TABLE 4 Hydrolysis products from 1% Avicel or CMC with *P. anserina* GH6 enzymes or *Tr*Cel6A, measured after 15 min (Avicel) and 24 h (Avicel and CMC) of hydrolysis under optimal conditions

Treatment and enzyme	Concn (μM)[a]				Processivity[b]
	Glucose	Cellobiose	Cellotriose	Total	
Avicel 15 min					
*Tr*Cel6A	9.2	112	5.7	127	
*Pa*Cel6A	7.5	57	5.9	71	
*Pa*Cel6B	3.3	32	4.5	40	
*Pa*Cel6C	3.6	23	2.7	30	
Avicel 24 h					
*Tr*Cel6A	246	2,119	0	2,365	7.6
*Pa*Cel6A	75	977	49	1,101	7.9
*Pa*Cel6B	43	283	8.3	335	4.7
*Pa*Cel6C	32	238	4.6	275	5.7
CMC 24 h					
*Tr*Cel6A	129	809	24	961	5.3
*Pa*Cel6A	12	355	69	436	4.4
*Pa*Cel6B	19	650	123	793	4.6
*Pa*Cel6C	4.4	142	16	162	7.1

[a] Values were determined by HPLC.

[b] For Avicel, processivity was calculated as the molar ratio (G2 − G1)/(G3 + G1), except for *Pa*Cel6A, where it was G2/(G1 + G3). For CMC, processivity was calculated as G2/(G3 + G1).

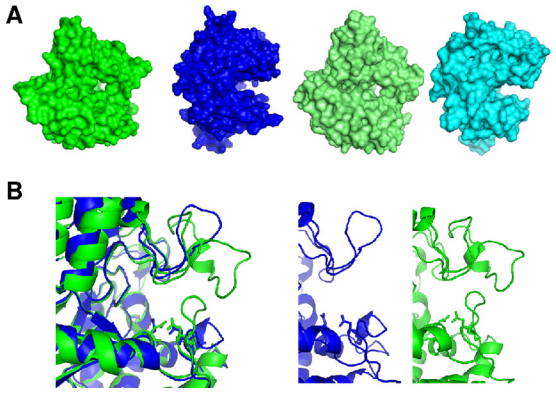

FIG 4 Structural analysis of *Pa*Cel6. (A) Surface representations of *Pa*Cel6A (left, in green), *Pa*Cel6B (middle left, in dark blue), *Pa*Cel6C (middle right, in light green), and *Pa*GH6D (right, in light blue). *Pa*Cel6A and *Pa*Cel6C (green) exhibit a tunnel formation, whereas *Pa*Cel6B and *Pa*GH6D show a cleft-shaped active site. (B) Structural alignment of the catalytic sites of *Pa*Cel6A (green) with *Pa*Cel6B (blue). The loop corresponding to amino acids 415 to 429 in *Pa*Cel6A leading to the formation of the tunnel shape is absent in *Pa*Cel6B. Models of *Pa*GH6 were built by using PHYRE2 and visualized with PyMOL. *Pa*Cel6A and *Pa*Cel6C models exhibited 100% confidence with *H. insolens* Cel6A (Protein Data Bank [PDB] accession numbers 1OC7 and 1BVW) and *Tr*Cel6A ((PDB accession number 1QJW), and *Pa*Cel6B and *Pa*GH6D models showed 100% confidence with *H. insolens* Cel6B (PDB accession number 1DYS).

[37]). With time, the ongoing processive hydrolysis might then lead to proportionally less G3 and G1 formation. Glucose thus seems to originate only from false initial attack, which is confirmed by the fact that *Pa*Cel6A, in contrast to *Tr*Cel6A, cannot cleave G3.

*Pa*Cel6B and *Pa*Cel6C produced small amounts of G3 and G1 after 15 min. G2/G3 ratios increased after 24 h for both enzymes, whereas G2/G1 ratios remained similar. As for *Tr*Cel6A, this is probably due to a slow hydrolysis of G3. The ratio of G2/(G1 + G3) or, for enzymes degrading G3, the ratio (G2 − G1)/(G3 + G1) can be used to estimate processivity (30). Table 4 shows that processivity was lower for *Pa*Cel6B and *Pa*Cel6C than for *Pa*Cel6A and *Tr*Cel6A.

All four tested enzymes were also able to hydrolyze CMC, with the highest activity observed for *Tr*Cel6A, followed by *Pa*Cel6B. *Tr*Cel6A released more glucose than G3, which is in contrast to the three *P. anserina* enzymes. A possible reason for this could be that *Tr*Cel6A slowly cleaves G3 into glucose and G2. Alternatively, more glucose than G3 could be produced by false initial attacks. The second hypothesis would be consistent with the fact that the bulkier side chains of CMC might have more difficulty in entering the tunnel-shaped active site. *Pa*Cel6A, *Pa*Cel6B, and *Pa*Cel6C produced more G3 than glucose, which is in contrast to the results obtained with Avicel at 24 h. Carboxymethyl cellotriose might not be a substrate for these enzymes. On the other hand, the rather high level of production of G3 by *Pa*Cel6A and *Pa*Cel6B may indicate a higher frequency of false initial attacks due to reduced processivity of these enzymes on CMC.

Endo- or exoglucanase activity? To gain information on the active-site topology of *P. anserina* Cel6 enzymes, homology models of all four *Pa*Cel6 enzymes were built based on known template 3D structures (Fig. 4). *Pa*Cel6A and *Pa*Cel6C display active-site tunnels, suggesting that they are processive enzymes, in good agreement with the biochemical data that demonstrate the highest activities on crystalline cellulose. The tunnel structure could also explain the lower activity on CMC, with the substituted glucose units having more difficulty entering the narrow active site. The processivity of *Pa*Cel6A on Avicel is similar to that of *Tr*Cel6A, suggesting that the types of action of the two enzymes could be similar. However, more work is needed to elucidate the reason for the lower catalytic efficiency and specific activity of *Pa*Cel6A. In contrast to *Pa*Cel6A and *Pa*Cel6C, the *Pa*Cel6B and *Pa*GH6D structures are predicted to contain a binding cleft rather than a tunnel structure. These two enzymes indeed lack 15 amino acids of the C-terminal loop (residues 406 to 420, according to *Tr*Cel6A numbering), generating an open topography of the active site. A similar short loop was also found for *H. insolens* Cel6B, an endoglucanase, which represents the closest characterized enzyme to *Pa*Cel6B and *Pa*GH6D, with 54 and 82% identity, respectively. Asn182 of the N-terminal loop, which is in direct contact with Arg410 of the C-terminal loop in exoglucanases (38), is also absent in the latter two enzymes (Fig. 2). The homology model thus supports the hypothesis that these enzymes have endo-type activity. In the case of *Pa*Cel6B, this was already suggested by the biochemical data obtained: higher activity on CMC than on Avicel and lower processivity on Avicel were found. In addition, this enzyme was shown to cleave glucomannan and β-(1,3;1,4)-glucan, suggesting that mixed hexose polymers with different β-linkages can be accommodated in the larger active site.

DISCUSSION

Since the 1960s, *P. anserina* has been used as a model for studying fundamental biological processes, such as life cycle and fungal sexual reproduction. Because this coprophilous fungus develops on herbivore dung after zygomycetes and (hemi)cellulose-degrading ascomycetes, it is believed to have to cope with the most recalcitrant plant residues. With the current intense search for efficient biomass conversion enzymes, *P. anserina* is beginning to be investigated for its biomass-degrading capacities. The publication of its genome indeed revealed a large portfolio of lignocellulose-degrading enzymes (17), which are only starting to be characterized (27). The present study is, to our knowledge, the first one describing cellulolytic enzymes of this organism.

P. pastoris has already been used successfully to express several *P. anserina* polysaccharide-degrading enzymes (27, 39) and numerous other CAZymes (40–42). In some cases, the heterologous proteins expressed in *P. pastoris* displayed a higher degree of glycosylation than their native counterparts (43–46), and this was also observed for *Tr*Cel6A and *Pa*Cel6A in the present study. Deglycosylation evidenced the presence of both *N*- and *O*-glycans in *Tr*Cel6A. However, *Pa*Cel6A could be only marginally deglycosylated. It is possible that the large number of *O*-glycosylation sites in the linker domain leads to glycan chains that are difficult to access, which might have prevented *O*-deglycosylation. The question arises as to whether enzymatic properties are affected by this high degree of glycosylation. Whereas glycosylation of CBM and catalytic domains can alter enzyme properties, such as activity and stability, glycosylation of the linker is generally considered to protect the enzyme from protease degradation (47). Concerning *Tr*Cel6A, glycosylation does not seem to alter its functioning; the specific activity of the recombinant *Tr*Cel6A enzyme on Avicel was similar to what was already reported in the literature, even if the experimental conditions were not strictly identical: 0.016

U/mg in this study, compared to 0.027 U/mg in studies by Tomme et al. (48) and Billard et al. (49), which were obtained with the native enzyme purified from *T. reesei*. The pH and temperature profiles of recombinant *Tr*Cel6A were also close to those previously obtained (50). It cannot be ruled out, however, that glycosylation or the presence of tags affects the biochemical properties of one of the heterologously produced *P. anserina* enzymes which could not be compared to their wild-type counterparts.

The pH and temperature profiles for the three *Pa*Cel6 enzymes were different from those for the recently described *P. anserina* hemicellulase enzymes (27). The GH6 enzymes studied here were generally less thermostable than the hemicellulases. In contrast, *Pa*Cel6 enzymes were active and stable in a much larger pH range, especially at alkaline pH, which was not observed for hemicellulases. Other fungal GH6 cellulases with alkaline pH optima have been described: *H. insolens* CBH2 (Cel6A) and *Magnaporthe oryzae* Cel6A show the highest activity at pH 9, but *H. insolens* Cel6B, an endoglucanase, has a much narrower pH optimum, centered at pH 7 (26, 51).

In contrast to *Pa*Cel6B and *Pa*Cel6C, *Pa*Cel6A harbors a CBM1 module at its N terminus. When adsorption was measured on Avicel, about 40% of the added enzymes were bound to cellulose at 4°C after 4 h, while *Pa*Cel6B and *Pa*Cel6C did not adsorb to the substrate (not shown), suggesting that *Pa*Cel6A-CBM1 is a functional CBM. The missing CBM in the latter two enzymes might also be the reason for the lower specific activities observed on Avicel. However, the CBM does not seem to be important for hydrolysis of CMC (a soluble substrate), as the specific activities are not correlated with its presence.

Modeling of the three-dimensional structures corroborated experimental data suggesting an endo or exo type of hydrolytic attack of *Pa*Cel6 enzymes. It has been known for quite some time, however, that the distinction between endo- and exoglucanases is not absolute and is sometimes hard to establish experimentally (16, 52–54). *H. insolens* Cel6A, a cellobiohydrolase, acts on crystalline cellulose ribbons in an endo-like fashion and hydrolyzes amorphous cellulose and CMC (26). However, its structure was shown to be very similar to that of *Tr*Cel6A, with two surface loops forming a substrate binding tunnel, characteristic of exoglucanases (38). Due to their ability to hydrolyze substituted glucose chains, such as CMC, both enzymes are therefore considered to be endo-processive cellobiohydrolases (24, 55). *Pa*Cel6C has a lower processivity on crystalline cellulose than does *Tr*Cel6A and hydrolyzes CMC nearly as well as crystalline cellulose. This suggests that this enzyme is better characterized as a processive glucanase with an even more pronounced endo character than the Cel6A enzyme of *T. reesei* or *H. insolens*.

Other examples of processive endoglucanases are known: *Agaricus bisporus* CEL3 possesses loops enclosing the active-site tunnel, but its activity profile was shown to be intermediate between typical cellobiohydrolases and endoglucanases (56). In prokaryotes, processive endoglucanases have been identified in *Saccharophagus degradans* (57), and a GH9 cellulase with both endo- and exoglucanase activities was described in *Cellulomonas fimi* (58).

The degree of endo-type activity can be related to different structural features, such as the structure of the catalytic core, which determines its binding strength (53). Binding of the substrate to the active site is known to involve several tryptophan residues (Trp135, Trp272, Trp367, and Trp269) (34). The most important one, Trp135, binds to the glucose unit at the −2 subsite, and its binding strength was demonstrated to drive the movement of the cellulose chain leading to processive cleavage (11). All of these residues are conserved in the *P. anserina* Cel6 enzymes, but different electrostatic environments at this subsite could lead to different degrees of processivity.

Active-site loops are another factor that may affect processivity. These are thought to display some flexibility and undergo conformational changes in response to ligand binding, which could lead to occasional endo cleavage even if the enzyme presents a tunnel-like structure (38, 59, 60). The cleavage of fluorescein-labeled cellodextrins by CBHs supports the hypothesis that such conformational changes occur (61). Therefore, the degree of flexibility and length of the active-site loops may also explain the different extents of endo action observed for the *Pa*Cel6 enzymes.

In a recent study, *P. anserina* secretomes that had been generated by induction with different substrates were tested for their capacity to supplement a *T. reesei* enzyme cocktail. By replacing half of the enzyme content with an equivalent amount of *P. anserina* enzymes, the hydrolysis yield of steam-exploded wheat straw could be increased up to 17% upon hydrolysis at 37°C. Proteomic analysis of the two secretomes that resulted in the highest gain of hydrolysis yield, namely, those obtained after induction by sugar beet pulp and Avicel, revealed the presence of the four *Pa*Cel6 enzymes: *Pa*Cel6A and *Pa*Cel6B were induced by both substrates, whereas *Pa*Cel6C and *Pa*GH6D were present in only one of the two secretomes (L. Poidevin, unpublished data). It cannot be confirmed at this point that the *Pa*Cel6 enzymes are responsible for the improvement in hydrolysis yield observed. However, this finding indicates that even though a *P. anserina* secretome hydrolyzes micronized or steam-pretreated wheat straw less efficiently than a *T. reesei* enzyme cocktail (Poidevin, unpublished), *P. anserina* produces enzymes which can effectively increase hydrolysis yields when added to a classical *Trichoderma* cellulase cocktail. We are only at the beginning of the characterization of the enzymatic complex of *P. anserina*, which includes about 180 genes encoding plant cell wall-degrading enzymes (17). The presence of 15 GH5 genes, 6 GH7 genes, encoding putative cellobiohydrolases, and 33 GH61 genes is particularly intriguing. Transcriptomic and proteomic studies are now under way to determine which enzymes are produced in the presence of lignocelluloses and to gain a deeper mechanistic understanding of the cell wall-degrading arsenal of this fungus.

ACKNOWLEDGMENTS

We thank M. Haon for her assistance with the expression of targets in *P. pastoris*.

This study was funded by the French National Research Agency (ANR) (program E-TRICEL ANR-07-BIOE-006).

REFERENCES

1. **Kleman-Leyer KM, Siika-Aho M, Teeri TT, Kirk TK.** 1996. The cellulases endoglucanase I and cellobiohydrolase II of *Trichoderma reesei* act synergistically to solubilize native cotton cellulose but not to decrease its molecular size. Appl. Environ. Microbiol. **62:**2883–2887.
2. **Nidetzky B, Steiner W, Hayn M, Claeyssens M.** 1994. Cellulose hydrolysis by the cellulases from *Trichoderma reesei*: a new model for synergistic interaction. Biochem. J. **298**(Part 3):705–710.
3. **Valjamae P, Sild V, Nutt A, Pettersson G, Johansson G.** 1999. Acid hydrolysis of bacterial cellulose reveals different modes of synergistic action between cellobiohydrolase I and endoglucanase I. Eur. J. Biochem. **266:**327–334.

4. **Henrissat B, Driguez H, Viet C, Schülein M.** 1985. Synergism of cellulases from *Trichoderma reesei* in the degradation of cellulose. Biotechnology **3:**722–726.
5. **Divne C, Stahlberg J, Reinikainen T, Ruohonen L, Pettersson G, Knowles JK, Teeri TT, Jones TA.** 1994. The three-dimensional crystal structure of the catalytic core of cellobiohydrolase I from *Trichoderma reesei*. Science **265:**524–528.
6. **Kleywegt GJ, Zou JY, Divne C, Davies GJ, Sinning I, Stahlberg J, Reinikainen T, Srisodsuk M, Teeri TT, Jones TA.** 1997. The crystal structure of the catalytic core domain of endoglucanase I from *Trichoderma reesei* at 3.6 Å resolution, and a comparison with related enzymes. J. Mol. Biol. **272:**383–397.
7. **Koivula A, Ruohonen L, Wohlfahrt G, Reinikainen T, Teeri TT, Piens K, Claeyssens M, Weber M, Vasella A, Becker D, Sinnott ML, Zou JY, Kleywegt GJ, Szardenings M, Stahlberg J, Jones TA.** 2002. The active site of cellobiohydrolase Cel6A from *Trichoderma reesei*: the roles of aspartic acids D221 and D175. J. Am. Chem. Soc. **124:**10015–10024.
8. **Lee TM, Farrow MF, Arnold FH, Mayo SL.** 2011. A structural study of *Hypocrea jecorina* Cel5A. Protein Sci. **20:**1935–1940.
9. **Rouvinen J, Bergfors T, Teeri T, Knowles JKC, Jones TA.** 1990. Three-dimensional structure of cellobiohydrolase II from *Trichoderma reesei*. Science **249:**380–386.
10. **Sandgren M, Shaw A, Ropp TH, Bott SWR, Cameron AD, Stahlberg J, Mitchinson C, Jones TA.** 2001. The X-ray crystal structure of the *Trichoderma reesei* family 12 endoglucanase 3, Cel12A, at 1.9 Å resolution. J. Mol. Biol. **308:**295–310.
11. **Varrot A, Frandsen TP, von Ossowski I, Boyer V, Cottaz S, Driguez H, Schulein M, Davies GJ.** 2003. Structural basis for ligand binding and processivity in cellobiohydrolase Cel6A from *Humicola insolens*. Structure **11:**855–864.
12. **Cantarel BL, Coutinho PM, Rancurel C, Bernard T, Lombard V, Henrissat B.** 2009. The Carbohydrate-Active EnZymes database (CAZy): an expert resource for glycogenomics. Nucleic Acids Res. **37:**D233–D238. doi:10.1093/nar/gkn663.
13. **Grassick A, Murray PG, Thompson R, Collins CM, Byrnes L, Birrane G, Higgins TM, Tuohy MG.** 2004. Three-dimensional structure of a thermostable native cellobiohydrolase, CBHIB, and molecular characterization of the *cel7* gene from the filamentous fungus, *Talaromyces emersonii*. Eur. J. Biochem. **271:**4495–4506.
14. **Munoz IG, Ubhayasekera W, Henriksson H, Szabo I, Pettersson G, Johansson G, Mowbray SL, Stahlberg J.** 2001. Family 7 cellobiohydrolases from *Phanerochaete chrysosporium*: crystal structure of the catalytic module of Cel7D (CBH58) at 1.32 Å resolution and homology models of the isozymes. J. Mol. Biol. **314:**1097–1111.
15. **Parkkinen T, Koivula A, Vehmaanpera J, Rouvinen J.** 2008. Crystal structures of *Melanocarpus albomyces* cellobiohydrolase Ce17B in complex with cello-oligomers show high flexibility in the substrate binding. Protein Sci. **17:**1383–1394.
16. **Teeri TT.** 1997. Crystalline cellulose degradation: new insight into the function of cellobiohydrolases. Trends Biotechnol. **15:**160–167.
17. **Espagne E, Lespinet O, Malagnac F, Da Silva C, Jaillon O, Porcel BM, Couloux A, Aury JM, Segurens B, Poulain J, Anthouard V, Grossetete S, Khalili H, Coppin E, Dequard-Chablat M, Picard M, Contamine V, Arnaise S, Bourdais A, Berteaux-Lecellier V, Gautheret D, de Vries RP, Battaglia E, Coutinho PM, Danchin EG, Henrissat B, El Khoury R, Sainsard-Chanet A, Boivin A, Pinan-Lucarre B, Sellem CH, Debuchy R, Wincker P, Weissenbach J, Silar P.** 2008. The genome sequence of the model ascomycete fungus *Podospora anserina*. Genome Biol. **9:**R77. doi:10.1186/gb-2008-9-5-r77.
18. **Martinez D, Berka RM, Henrissat B, Saloheimo M, Arvas M, Baker SE, Chapman J, Chertkov O, Coutinho PM, Cullen D, Danchin EG, Grigoriev IV, Harris P, Jackson M, Kubicek CP, Han CS, Ho I, Larrondo LF, de Leon AL, Magnuson JK, Merino S, Misra M, Nelson B, Putnam N, Robbertse B, Salamov AA, Schmoll M, Terry A, Thayer N, Westerholm-Parvinen A, Schoch CL, Yao J, Barbote R, Nelson MA, Detter C, Bruce D, Kuske CR, Xie G, Richardson P, Rokhsar DS, Lucas SM, Rubin EM, Dunn-Coleman N, Ward M, Brettin TS.** 2008. Genome sequencing and analysis of the biomass-degrading fungus *Trichoderma reesei* (syn. *Hypocrea jecorina*). Nat. Biotechnol. **26:**553–560.
19. **Zhang YH, Lynd LR.** 2004. Toward an aggregated understanding of enzymatic hydrolysis of cellulose: noncomplexed cellulase systems. Biotechnol. Bioeng. **88:**797–824.
20. **Reese ET, Mandels M.** 1980. Stability of the cellulase of *Trichoderma reesei* under use conditions. Biotechnol. Bioeng. **22:**323–335.
21. **Herpoel-Gimbert I, Margeot A, Dolla A, Jan G, Molle D, Lignon S, Mathis H, Sigoillot JC, Monot F, Asther M.** 2008. Comparative secretome analyses of two *Trichoderma reesei* RUT-C30 and CL847 hypersecretory strains. Biotechnol. Biofuels **1:**18. doi:10.1186/1754-6834-1-18.
22. **Rosgaard L, Pedersen S, Langston J, Akerhielm D, Cherry JR, Meyer AS.** 2007. Evaluation of minimal *Trichoderma reesei* cellulase mixtures on differently pretreated barley straw substrates. Biotechnol. Prog. **23:**1270–1276.
23. **Suominen PL, Mantyla AL, Karhunen T, Hakola S, Nevalainen H.** 1993. High frequency one-step gene replacement in *Trichoderma reesei*. II. Effects of deletions of individual cellulase genes. Mol. Gen. Genet. **241:**523–530.
24. **Boisset C, Fraschini C, Schulein M, Henrissat B, Chanzy H.** 2000. Imaging the enzymatic digestion of bacterial cellulose ribbons reveals the endo character of the cellobiohydrolase Cel6A from *Humicola insolens* and its mode of synergy with cellobiohydrolase Cel7A. Appl. Environ. Microbiol. **66:**1444–1452.
25. **Davies GJ, Brzozowski AM, Dauter M, Varrot A, Schulein M.** 2000. Structure and function of *Humicola insolens* family 6 cellulases: structure of the endoglucanase, Cel6B, at 1.6 Å resolution. Biochem. J. **348:**201–207.
26. **Schulein M.** 1997. Enzymatic properties of cellulases from *Humicola insolens*. J. Biotechnol. **57:**71–81.
27. **Couturier M, Haon M, Coutinho PM, Henrissat B, Lesage-Meessen L, Berrin JG.** 2011. Podospora anserina hemicellulases potentiate the *Trichoderma reesei* secretome for saccharification of lignocellulosic biomass. Appl. Environ. Microbiol. **77:**237–246.
28. **Navarro D, Couturier M, da Silva GGD, Berrin JG, Rouau X, Asther M, Bignon C.** 2010. Automated assay for screening the enzymatic release of reducing sugars from micronized biomass. Microb. Cell Fact. **9:**58. doi:10.1186/1475-2859-9-58.
29. **Heiss-Blanquet S, Zheng D, Ferreira NL, Lapierre C, Baumberger S.** 2011. Effect of pretreatment and enzymatic hydrolysis of wheat straw on cell wall composition, hydrophobicity and cellulase adsorption. Bioresour. Technol. **102:**5938–5946.
30. **Vuong TV, Wilson DB.** 2009. Processivity, synergism, and substrate specificity of *Thermobifida fusca* Cel6B. Appl. Environ. Microbiol. **75:**6655–6661.
31. **von Ossowski I, Stahlberg J, Koivula A, Piens K, Becker D, Boer H, Harle R, Harris M, Divne C, Mahdi S, Zhao Y, Driguez H, Claeyssens M, Sinnott ML, Teeri TT.** 2003. Engineering the Exo-loop of *Trichoderma reesei* cellobiohydrolase, Cel7A. A comparison with *Phanerochaete chrysosporium* Cel7D. J. Mol. Biol. **333:**817–829.
32. **Park JT, Johnson MJ.** 1949. A submicrodetermination of glucose. J. Biol. Chem. **181:**149–151.
33. **Kelley LA, Sternberg MJE.** 2009. Protein structure prediction on the Web: a case study using the Phyre server. Nat. Protoc. **4:**363–371.
34. **Koivula A, Reinikainen T, Ruohonen L, Valkeajarvi A, Claeyssens M, Teleman O, Kleywegt GJ, Szardenings M, Rouvinen J, Jones TA, Teeri TT.** 1996. The active site of *Trichoderma reesei* cellobiohydrolase II: the role of tyrosine 169. Protein Eng. **9:**691–699.
35. **Davies GJ, Wilson KS, Henrissat B.** 1997. Nomenclature for sugar-binding subsites in glycosyl hydrolases. Biochem. J. **321:**557–559.
36. **Harjunpää V, Teleman A, Koivula A, Ruohonen L, Teeri TT, Teleman O, Drakenberg T.** 1996. Cello-oligosaccharide hydrolysis by cellobiohydrolase II from *Trichoderma reesei*. Eur. J. Biochem. **240:**584–591.
37. **Medve J, Karlsson J, Lee D, Tjerneld F.** 1998. Hydrolysis of microcrystalline cellulose by cellobiohydrolase I and endoglucanase II from *Trichoderma reesei*: adsorption, sugar production pattern, and synergism of the enzymes. Biotechnol. Bioeng. **59:**621–634.
38. **Varrot A, Hastrup S, Schulein M, Davies GJ.** 1999. Crystal structure of the catalytic core domain of the family 6 cellobiohydrolase II, Cel6A, from *Humicola insolens*, at 1.92 Å resolution. Biochem. J. **337:**297–304.
39. **Bey M, Zhou S, Poidevin L, Henrissat B, Coutinho PM, Berrin JG, Sigoillot JC.** 2013. Cello-oligosaccharide oxidation reveals differences between two lytic polysaccharide monooxygenases (family GH61) from *Podospora anserina*. Appl. Environ. Microbiol. **79:**488–496.
40. **Bauer S, Vasu P, Persson S, Mort AJ, Somerville CR.** 2006. Development and application of a suite of polysaccharide-degrading enzymes for analyzing plant cell walls. Proc. Natl. Acad. Sci. U. S. A. **103:**11417–11422.
41. **Chen X, Cao Y, Ding Y, Lu W, Li D.** 2007. Cloning, functional expres-

sion and characterization of *Aspergillus sulphureus* beta-mannanase in *Pichia pastoris*. J. Biotechnol. **128:**452–461.
42. **He J, Yu B, Zhang KY, Ding XM, Chen DW.** 2009. Expression of endo-1,4-beta-xylanase from *Trichoderma reesei* in *Pichia pastoris* and functional characterization of the produced enzyme. BMC Biotechnol. **9:**56. doi:10.1186/1472-6750-9-56.
43. **Akcapinar GB, Gul O, Sezerman UO.** 2012. From in silico to in vitro: modelling and production of *Trichoderma reesei* endoglucanase 1 and its mutant in *Pichia pastoris*. J. Biotechnol. **159:**61–68.
44. **Bey M, Berrin JG, Poidevin L, Sigoillot JC.** 2011. Heterologous expression of *Pycnoporus cinnabarinus* cellobiose dehydrogenase in *Pichia pastoris* and involvement in saccharification processes. Microb. Cell Fact. **10:**113. doi:10.1186/1475-2859-10-113.
45. **Boer H, Teeri TT, Koivula A.** 2000. Characterization of *Trichoderma reesei* cellobiohydrolase CeI7A secreted from *Pichia pastoris* using two different promoters. Biotechnol. Bioeng. **69:**486–494.
46. **Boonvitthya N, Bozonnet S, Burapatana V, O'Donohue MJ, Chulalaksananukul W.** 2013. Comparison of the heterologous expression of *Trichoderma reesei* endoglucanase II and cellobiohydrolase II in the yeasts *Pichia pastoris* and *Yarrowia lipolytica*. Mol. Biotechnol. **54:**158–169.
47. **Langsford ML, Gilkes NR, Singh B, Moser B, Miller RC, Jr, Warren RAJ, Kilburn DG.** 1987. Glycosylation of bacterial cellulases prevents proteolytic cleavage between functional domains. FEBS Lett. **225:**163–167.
48. **Tomme P, Vantilbeurgh H, Pettersson G, Vandamme J, Vandekerckhove J, Knowles J, Teeri T, Claeyssens M.** 1988. Studies of the cellulolytic system of *Trichoderma reesei* Qm-9414—analysis of domain function in 2 cellobiohydrolases by limited proteolysis. Eur. J. Biochem. **170:**575–581.
49. **Billard H, Faraj A, Ferreira NL, Menir S, Heiss-Blanquet S.** 2012. Optimization of a synthetic mixture composed of major *Trichoderma reesei* enzymes for the hydrolysis of steam-exploded wheat straw. Biotechnol. Biofuels **5:**9. doi:10.1186/1754-6834-5-9.
50. **Okada H, Sekiya T, Yokoyama K, Tohda H, Kumagai H, Morikawa Y.** 1998. Efficient secretion of *Trichoderma reesei* cellobiohydrolase II in *Schizosaccharomyces pombe* and characterization of its products. Appl. Microbiol. Biotechnol. **49:**301–308.
51. **Takahashi M, Takahashi H, Nakano Y, Konishi T, Terauchi R, Takeda T.** 2010. Characterization of a cellobiohydrolase (MoCel6A) produced by *Magnaporthe oryzae*. Appl. Environ. Microbiol. **76:**6583–6590.
52. **Kyriacou A, Mackenzie CR, Neufeld RJ.** 1987. Detection and characterization of the specific and nonspecific endoglucanases of *Trichoderma reesei*—evidence demonstrating endoglucanase activity by cellobiohydrolase-II. Enzyme Microb. Technol. **9:**25–32.
53. **Stahlberg J, Johansson G, Pettersson G.** 1993. *Trichoderma reesei* has no true exo-cellulase—all intact and truncated cellulases produce new reducing end groups on cellulose. Biochim. Biophys. Acta **1157:**107–113.
54. **Henrissat B, Davies G.** 1997. Structural and sequence-based classification of glycoside hydrolases. Curr. Opin. Struct. Biol. **7:**637–644.
55. **Medve J, Stahlberg J, Tjerneld F.** 1994. Adsorption and synergism of cellobiohydrolase-I and cellobiohydrolase-II of *Trichoderma reesei* during hydrolysis of microcrystalline cellulose. Biotechnol. Bioeng. **44:**1064–1073.
56. **Chow CM, Yague E, Raguz S, Wood DA, Thurston CF.** 1994. The Cel3 gene of *Agaricus bisporus* codes for a modular cellulase and is transcriptionally regulated by the carbon source. Appl. Environ. Microbiol. **60:**2779–2785.
57. **Watson BJ, Zhang HT, Longmire AG, Moon YH, Hutcheson SW.** 2009. Processive endoglucanases mediate degradation of cellulose by *Saccharophagus degradans*. J. Bacteriol. **191:**5697–5705.
58. **Tomme P, Kwan E, Gilkes NR, Kilburn DG, Warren RAJ.** 1996. Characterization of CenC, an enzyme from *Cellulomonas fimi* with both endo- and exoglucanase activities. J. Bacteriol. **178:**4216–4223.
59. **Henrissat B, Teeri TT, Warren RA.** 1998. A scheme for designating enzymes that hydrolyse the polysaccharides in the cell walls of plants. FEBS Lett. **425:**352–354.
60. **Zou JY, Kleywegt GJ, Stahlberg J, Driguez H, Nerinckx W, Claeyssens M, Koivula A, Teeri TT, Jones TA.** 1999. Crystallographic evidence for substrate ring distortion and protein conformational changes during catalysis in cellobiohydrolase Cel6A from *Trichoderma reesei*. Structure **7:**1035–1045.
61. **Armand S, Drouillard S, Schulein M, Henrissat B, Driguez H.** 1997. A bifunctionalized fluorogenic tetrasaccharide as a substrate to study cellulases. J. Biol. Chem. **272:**2709–2713.